PCCP

Impact of Intrinsic Framework Flexibility for Selective Adsorption of Sarin in Non-Aqueous Solvents using Metal-Organic Frameworks

Journal:	*Physical Chemistry Chemical Physics*
Manuscript ID	CP-ART-12-2019-006788.R1
Article Type:	Paper
Date Submitted by the Author:	13-Feb-2020

Complete List of Authors:	Park, Jongwoo; Georgia Institute of Technology, School of Chemical & Biomolecular Engineering Agrawal, Mayank; Georgia Institute of Technology College of Engineering, Chemical Engineering Sava Gallis, Dorina; Sandia National Laboratories, Department of Nanoscale Sciences Harvey, Jacob; Sandia National Laboratories, Geochemistry Greathouse, Jeffery; Sandia National Laboratories, Geochemistry Department Sholl, David; Georgia Institute of Technology, School of Chemical andBiomolecular Engineering

Impact of Intrinsic Framework Flexibility for Selective Adsorption of Sarin in Non-Aqueous Solvents using Metal-Organic Frameworks

Jongwoo Park[1], Mayank Agrawal[1], Dorina F. Sava Gallis[2], Jacob A. Harvey[3], Jeffery A. Greathouse[3], and David S. Sholl[1*]

[1] School of Chemical & Biomolecular Engineering, Georgia Institute of Technology, Atlanta, GA 30332 USA

[2] Nanoscale Sciences Department, Sandia National Laboratories, Albuquerque, NM 87185 USA

[3] Geochemistry Department, Sandia National Laboratories, Albuquerque, NM 87185 USA

[*] Corresponding author. E-mail: david.sholl@chbe.gatech.edu.

ABSTRACT

Molecular modeling of mixture adsorption in nanoporous materials can provide insight into the molecular-level details that underlie adsorptive separations. Modeling of adsorption often employs a rigid framework approximation for computational convenience. All real materials, however, have intrinsic flexibility due to thermal vibrations of their atoms. In this article, we examine quantitative predictions of the adsorption selectivity for a dilute concentration of a chemical warfare agent, sarin, from bulk mixtures with aqueous and non-aqueous (methanol, isopropyl alcohol) solvents using metal-organic frameworks (MOFs). These predictions were made in MOFs approximated as rigid and also in MOFs allowed to have intrinsic flexibility. Including framework flexibility appears to have important consequences for quantitative predictions of adsorption selectivity, particularly for sarin/water mixtures. Our observations suggest the intrinsic flexibility of MOFs can have a nontrivial impact on adsorption modeling of molecular mixtures, specifically for mixtures containing polar species and molecules of different sizes.

1. INTRODUCTION

Due to the extremely toxic properties of chemical warfare agents (CWAs)[1,2], efforts have been made to develop methods and materials for the detection and destruction of CWAs[3-5]. Sarin, for instance, is an organophosphorous nerve agent, one of the major categories of CWAs.[6,7] Catalytic degradation of CWAs into less toxic compounds using porous materials is a viable method of decontaminating these agents.[3-10] Activated carbon and metal oxides have been widely investigated for this purpose, but finding alternative types of protective materials is of significant interest.[2,3] Metal-organic frameworks (MOFs) have emerged as promising candidates due to their large pores that enable easy access of CWAs to internal catalytic sites.[4-10] Nonetheless, an efficient detoxification procedure for CWAs in porous materials can only be possible if CWAs are selectively captured in those materials.[11,12] It is therefore useful to consider adsorption properties of CWAs before their catalytic activity is examined.

The majority of studies of catalytic degradation of CWAs to date have focused on hydrolysis.[13-19] Nucleophilic water substitutes at the phosphorus atom of the agent which leads to elimination of the toxic leaving group.[17-20] Nevertheless, situations exist where hydrolysis reactions are not appropriate. The damage-free decontamination of electronics after exposure to CWAs, for example, is incompatible with hydrolysis.[21] This motivates interest in the detection and detoxification of CWAs in non-aqueous solvents.[21-24] Recent modeling efforts have indicated that the displacement of solvent molecules at the active sites of porous materials can be a rate limiting step in CWA degradation.[17-19] Therefore, desigining materials that selectively adsorb CWAs from co-existing solvents is of critical importance. In this context we seek to examine the selective adsorption of sarin in the nanopores of MOFs in the presence of a range of solvents.

Molecular modeling has been used to predict the adsorption properties of a variety of adsorbing molecules in a wide range of MOFs.[25-29] Adsorption modeling of this kind, often referred to as high-throughput materials screening, almost always assumes that the MOF structure can be held rigid during simulation of adsorption, an assumption that leads to very significant computational efficiencies. This approximation assumes that the relaxation of the framework atoms due to the presence of adsorbed molecules can be neglected.[30-33] Although there are classes of MOFs that undergo significant adsorption-induced deformations, including swelling and transitions between bistable states,[34] there are also many MOFs that can be reasonably expected to have little or no volume change in response to adsorption ($\Delta V = 0$). In all

MOFs, however, and indeed in all materials, thermal vibrations cause atoms to move with small displacements.[35-37] We refer to these movements as the intrinsic flexibility of the adsorbent. Several recent studies have shown that this intrinsic flexibility can in some cases have a nontrivial impact on the predictions of molecular modeling of adsorption in MOFs.[38-41]

In this article, we examine the adsorption of sarin in MOFs in the presence of water, methanol, and isopropyl alcohol via molecular simulations for a collection of 23 sarin-selective hydrophobic MOFs. In each material, we examined the impact of intrinsic flexibility with $\Delta V = 0$ on adsorption selectivity. Our findings provide insight on the impact of this kind of flexibility on mixture adsorption when molecular mixtures consist of adsorbates of different polarities and sizes which, to our best knowledge, has not been examined before.

2. COMPUTATIONAL METHODS

2.1. MOF selection criteria and bulk mixture conditions

We selected a set of adsorbent materials from a large collection of experimentally known MOFs. A subset of the CoRE MOF database[42] for which high-quality atomic point charges have been assigned[43] contains 2932 crystal structures. It has been reported that Zr-based UiO-66 and its derivatives are effective catalysts for sarin degradation.[14-19,44,45] We therefore also considered UiO-66 and 36 UiO-66 derivatives with distinctive functional groups.[46] The same type of atomic point charges as for the CoRE MOF database have been assigned previously to these frameworks.[46] This gave an initial set of 2969 MOFs.

Because it is computationally intensive to carry out molecular simulations for adsorption of bulky molecules in MOFs with intrinsic flexibility, we needed to reduce the number of materials. The material selection criteria used in this work is illustrated in Fig. 1. We aimed to find CWA-selective, hydrophobic MOFs with sufficient pore size to admit sarin. 2469 structures were first chosen from the initial set that have largest cavity diameters larger than 4 Å, indicating a sufficient pore size to admit sarin. We then selected CWA-selective hydrophobic MOFs in order to find materials that would be suitable for CWA capture under humid conditions. To do so, we used the constraints of Henry constants (K_H) as suggested in similar earlier work by Matito-Martos et al.[11,47] We calculated room temperature Henry constants for sarin and soman, another extensively studied nerve agent[1-3], ($K_{H,CWA}$) and that for water ($K_{H,H2O}$) using methods defined

further below. Including information about the adsorption affinity of soman gives a more general perspective on finding CWA-selective materials candidates, although below we exclusively examine the adsorption of sarin. We retained only those MOFs for which $K_{H,CWA}$ was larger than 10^{-3} mol/kg·Pa for both sarin and soman and also had $K_{H,H2O}$ less than 10^{-5} mol/kg·Pa. This selection procedure resulted in 23 MOFs. More information about these 23 materials is given in the Electronic Supplementary Information (ESI) (Table S1).

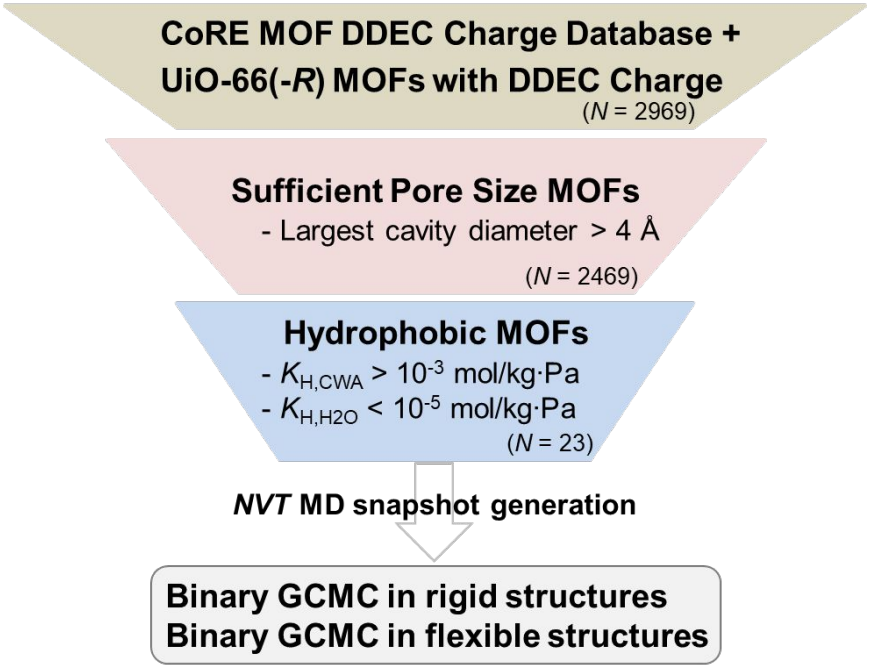

Fig. 1. Schematic illustration of the MOF selection strategy. The number of MOFs at each stage are shown in brackets (*N*).

We explored the adsorption of sarin in the presence of three solvents at 298 K, sarin/water (H_2O), sarin/methanol (MeOH), and sarin/isopropyl alcohol (IPA). The mixture compositions in the bulk phase were defined by the partial pressures of sarin (P_{sarin}) and each solvent *i* (P_i). To represent a dilute concentration of sarin in solvent saturated environments, we set P_{sarin} = 0.001 bar in mixtures with P_i set to the saturation pressure of each solvent (P^0_i). The adsorption selectivity for sarin (*S*) was then calculated at total pressures of each mixture as defined in Eq. (1)[48] where N_{sarin} and N_i refer to adsorbed amounts of sarin and solvents, respectively, in either rigid or intrinsically flexible MOFs predicted from mixture adsorption simulations. Fig. 2 shows atomic representations of sarin and the solvent molecules.

$$S = \frac{N_{sarin}/N_i}{P_{sarin}/P_i} \qquad (1)$$

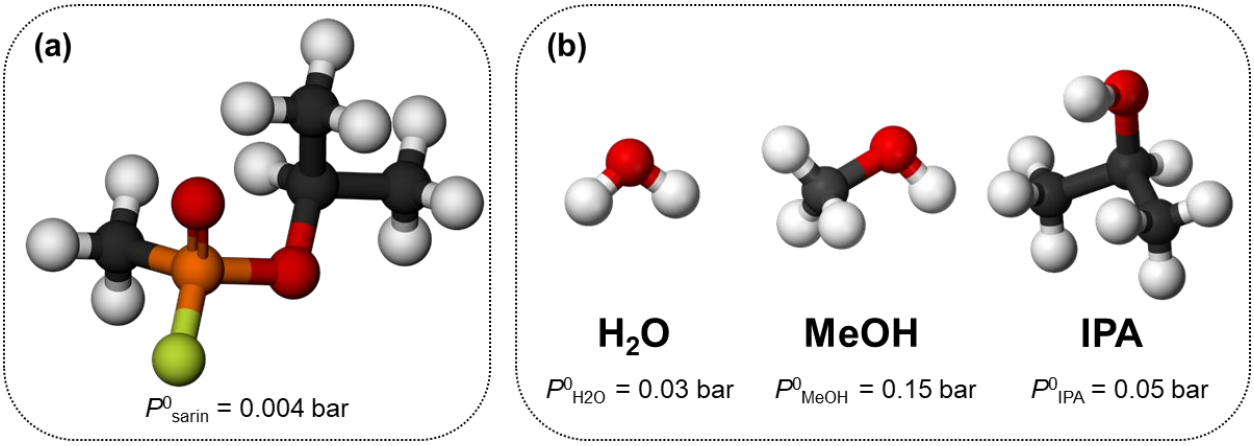

Fig. 2. Atomic representations of (a) sarin and (b) solvent molecules. Carbon, oxygen, hydrogen, phosphorus, and fluorine are shown in black, red, white, orange, and yellow, respectively. Room temperature saturation pressures for each molecule that were used to determine the bulk mixture compositions are also shown. P^0_{sarin} is taken from the literature[2] and $P^0_{solvent}$ were defined using the Antoine equation[49] at 298 K.

2.2. Flexible snapshot method

We performed simulations allowing intrinsic flexibility for the 23 MOFs chosen above. The flexible snapshot method first introduced by Gee et al.[40] was used to generate an ensemble of empty MOF frameworks by simulating the dynamics of each MOF.[41] *NVT* molecular dynamics (MD) simulations were conducted after structure relaxation using classical force fields[50] in LAMMPS[51] at 300 K with a time step of 1.0 fs. Each MOF was described using the UFF4MOF force field of Coupry et al.[50] The temperature was controlled via a Nosé-Hoover thermostat with a 0.1 ps decay period. As a result, *NVT* MD snapshots were generated that represent intrinsically flexible empty MOFs. This method cannot capture aspects of flexibility that might arise due to coupling with adsorbate degrees of freedom.[41] Adsorption in the flexible material was characterized by averaging independent Grand Canonical Monte Carlo (GCMC) simulations of structures generated from snapshots of empty MOF structures. Each snapshot was held rigid during these GCMC simulations.

The computational cost of the flexible snapshot method is proportional to the number of *NVT* MD snapshots employed for GCMC calculations. To this end, selecting uncorrelated MD snapshots from each structure is important.[41] In this work, MD snapshots were taken every 100 ps from a production period of 1 ns, which is consistent with the recent work of Agrawal et al.[41]

In principle it would also be possible to use *ab initio* MD as an alternative method to generate framework snapshots.[52,53] This method, however, is even more computationally demanding than classical simulations we have used here.

2.3. Adsorption modeling of rigid and intrinsically flexible MOFs

Molecular modeling of adsorption of binary molecular mixtures in MOFs was conducted with GCMC simulations using RASPA.[54,55] MOF structures reported by the CoRE MOF database and a set of UiO-66 derivatives were first relaxed using the modified generic force field for MOFs reported as UFF4MOF force field[50] in LAMMPS[51] followed by fixing the atoms in the relaxed structures. We refer to these structures as rigid MOFs while carrying out GCMC simulations. GCMC simulations were also performed independently in the snapshots generated for each structure as described above; we refer to these results below as coming from flexible MOFs. To perform GCMC calculations, appropriate force fields are needed to describe non-bonding interactions such as van der Waals and Coulombic interactions for adsorbate/adsorbent and adsorbate/adsorbate interactions. Standard force fields, i.e. the UFF[56] and the TraPPE[57] force field, that are reasonably well justified for adsorption modeling[25-27] were used to compute van der Waals interactions. Lennard-Jones parameters for MOF atoms and sarin, solvent molecules were taken from UFF and TraPPE force field, respectively. Adsorbate/adsorbent interactions were defined with Lorentz-Berthelot mixing rules.[58] Periodic boundary conditions were defined in all dimensions and adsorbates were approximated as rigid. Coulombic interactions were modeled pairwise with a long-range Ewald summation scheme.[59] These interactions are computed via the DDEC point charges for MOF atoms[60-62] and TraPPE charges for sarin and solvent molecules[54,55]. Attempted Monte Carlo moves include translation, rotation, regrowth, reinsertion, deletion, and insertion of adsorbates with identical probabilities. In addition, a Monte Carlo move that swapped the identity of adsorbed molecules was used.

Henry constants, K_H, for sarin, soman, and water used as a material selection criteria as discussed in Section 2.1 were computed via a Widom particle insertion method[63] with the force fields just discussed. All K_H calculations were performed at 298 K in rigid MOFs only. K_H data for all MOFs considered in Fig. 1 are provided in Table S2.

Using the flexible snapshot method, the adsorption properties of intrinsically flexible MOFs are approximated by performing independent GCMC simulations in distinct MOF structures

taken from MD snapshots. The adsorption data were then averaged over GCMC results from each MD snapshot. We used 10 snapshots for each material. Agrawal et al.[41] previously showed that this was sufficient to achieve converged results.

3. RESULTS AND DISCUSSION

3.1. Selective adsorption of sarin in non-/aqueous environments

Our discussion focuses on adsorption selectivity for sarin at conditions corresponding to the liquid state for each solvent. This means that the MOFs were typically highly loaded with solvent molecules (see Fig. S1). The computed adsorption selectivity for sarin in the 23 MOFs at 298 K by employing the rigid framework approximation, S_{Rigid}, is shown in Fig. 3. As might be expected, chosen MOFs were selective for sarin in every co-adsorbed solvent. This suggests they could be effective for catalytic degradation of sarin, assuming of course that catalytically active sites can be created and that the energy barriers to displace solvent from these sites are sufficiently low[17-19] in each material.

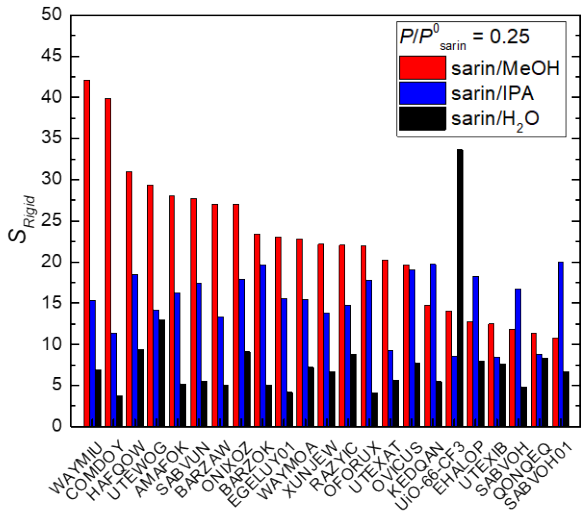

Fig. 3. Adsorption selectivity for sarin calculated via binary mixture GCMC in rigid approximations of 23 MOFs for each molecular mixture at bulk pressure of $P_{total} = P_{sarin} + P_{solvents}$ at 298 K. Mixture compositions in the bulk phase were defined to give a partial pressure of sarin of $P/P^0_{sarin} = 0.25$ and a solvent partial pressure of $P/P^0_{solvent} = 1$. MOFs are listed in order of decreasing sarin selectivity in the sarin/MeOH mixture.

In almost every MOF, the sarin adsorption selectivity was larger for the non-aqueous solvents

than for H_2O. This trend is reasonable, specifically for the comparison between non-aqueous and aqueous mixtures, because the non-aqueous molecules are larger than H_2O and also typically have weaker adsorption affinity as characterized by K_H (Table S2). Meanwhile, there exists a competition between solvent/MOF (measured by K_H, Table S2) and solvent/solute (measured by polarity index, Table S3) interactions. In MeOH the solvent/solute interaction outweighs the solvent/MOF interaction, however in IPA this is not always the case. In most, but not all, MOFs the weaker solvent/solute interaction plays a large role and leads to a greater adsorption of the solvent than sarin in the MOF, and therefore lower adsorption selectivity for sarin/IPA mixtures than for sarin/MeOH mixtures. This is also corroborated by the experimentally observed lower reactivity of sarin in IPA.[64]

3.2. Impact of intrinsic MOF flexibility on mixture adsorption modeling

We repeated the GCMC simulations of adsorption of sarin-containing binary mixtures allowing intrinsic flexibility of the MOFs with $\Delta V = 0$ using the flexible snapshot method. To examine the convergence of our flexible snapshot method with respect to the number of snapshots used, the deviation in the loadings of adsorbing molecules and sarin adsorption selectivities in distinct snapshots are shown in a representative MOF in Fig. S2. The differences between snapshots in the loadings and selectivities are relatively small, even though these properties differ markedly from the rigid structure MOF. This suggests that using 10 independent snapshots as we have throughout our calculations is sufficient to achieve converged results.

Fig. 4 compares the computed selectivities from rigid and flexible representations of the MOFs. An immediate observation is that for many of the MOFs there is a clear quantitative discrepancy between the two calculations for all three sarin-containing mixtures. Modeling the MOFs as rigid tends to underestimate the adsorption selectivity, although there are exceptions to this description. In most cases, the increased selectivity in the flexible MOFs was associated with higher adsorbed amounts of sarin and lower adsorbed amounts of the solvent than in the rigid MOF. When the selectivity from the flexible calculation was less than that from the rigid calculation, sarin adsorption was typically reduced with little change in the solvent loading. Similar to results with rigid MOFs, sarin is more selectively adsorbed in non-aqueous solvents in flexible MOFs (see also Fig. S3).

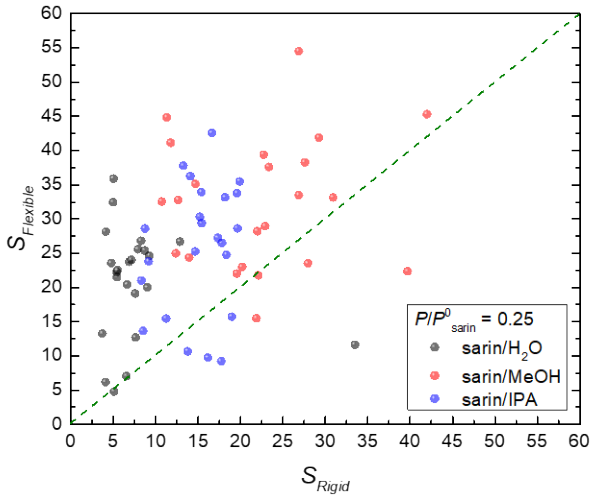

Fig. 4. Parity plot of adsorption selectivities predicted at 298 K in 23 MOFs approximated as rigid (horizontal axis) and allowed to have intrinsic flexibility (vertical axis) for each molecular mixture. The parity line indicates the result that would be obtained if there was no effect of intrinsic flexibility.

As noted above, typical high-throughput screening approaches of MOFs or other porous adsorbents rely on the rigid framework approximation because of its computational efficiency. One common goal of material screening is to rank a large number of materials. It is therefore useful to ask whether rankings of MOFs based on rigid and flexible calculations are similar for the sarin mixtures we studied. We approached this by calculating Spearman's rank-order correlation, ρ, to the rankings for sarin/H_2O, sarin/MeOH and sarin/IPA selectivities from rigid and flexible calculations.[65,66] This ranking can vary between -1 and 1, with values of -1, 0 and 1 corresponding to rankings that are anti-correlated, uncorrelated and completely correlated, respectively. For the 23 materials we studied, ρ for sarin/H_2O was 0.08, for sarin/MeOH was 0.15 and for sarin/IPA was 0.23. These values show there is little correlation between the two MOF rankings[65] with respect to adsorption selectivity provided by rigid and flexible calculations. To illustrate this differently, the three most selective MOFs from our set of 23 for sarin/MeOH as predicted using rigid structures have CSD reference codes WAYMIU, COMDOY and HAFQOW (see Fig. 3). However, in our intrinsically flexible calculations, these three MOFs ranked 2nd, 20th and 11th for sarin/MeOH selectivity. Earlier work by Gee et al.[40] suggested that simulations based on flexible MOFs as we have performed here give more reliable predictions than simulations based on rigid MOFs. This observation suggests that attempting to accurately

select a handful of the "best" MOFs for sarin separation based on rigid structure calculations may be difficult. It is important to note, however, that the rigid calculations do correctly describe key trends in CWA adsorption. That said, both the rigid and flexible structure calculations predict that sarin selectivity as a function of solvent follows the general trend sarin/MeOH > sarin/IPA > sarin/H_2O mixtures.

Fig. 5 shows a histogram of MOFs as a function of $S_{Flexible}/S_{Rigid}$ for each mixture. For sarin/MeOH and sarin/IPA, the rigid MOF calculations underestimate the result from the flexible materials by 60-70%, on average. Meanwhile, the rigid MOFs overpredict the selectivity in 17% of materials. For sarin/H_2O, however, the rigid MOFs underestimate the selectivity by an average of 322%. The variability in the difference between the rigid and flexible calculations is more marked for aqueous mixtures than non-aqueous mixtures. Three of the 23 MOFs we examined showed more than 600% higher selectivity for sarin/H_2O in the flexible calculations, while for two MOFs the selectivity for the same mixture was overestimated by the rigid MOF calculation.

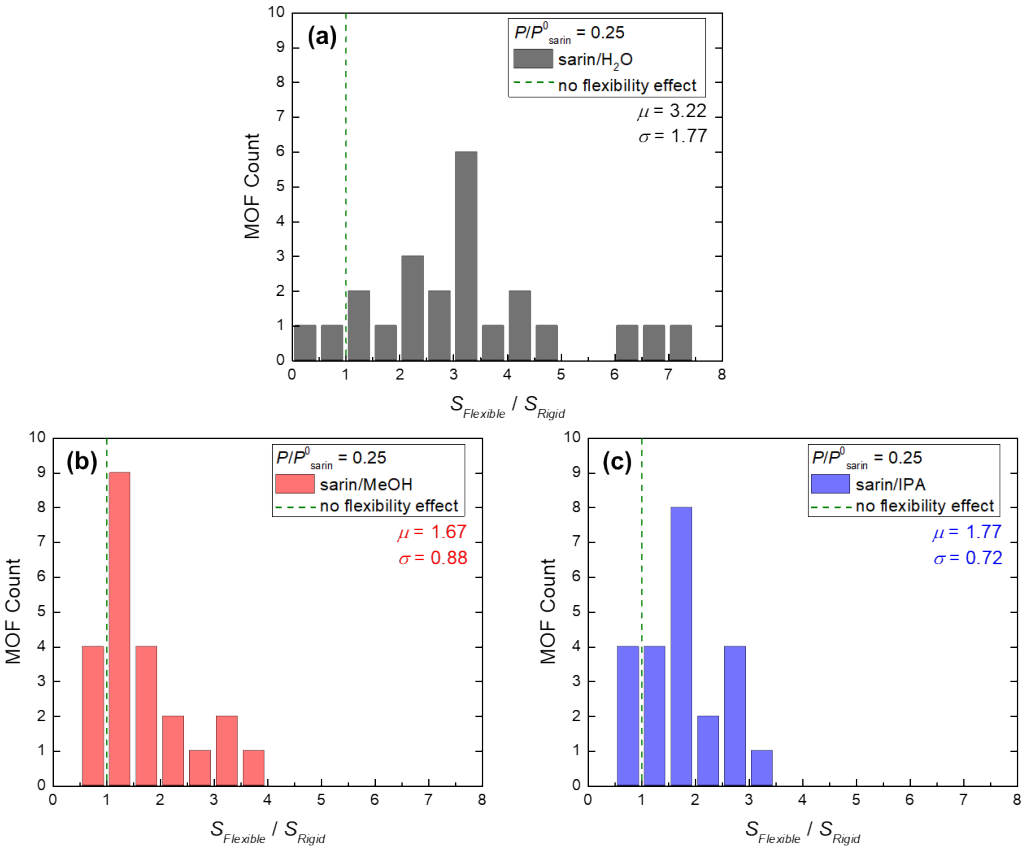

Fig. 5. Histogram plots showing the number of MOFs observed as a function of $S_{Flexible}/S_{Rigid}$ in each mixture of (a) sarin/H_2O, (b) sarin/MeOH, and (c) sarin/IPA. Green dashed lines show

$S_{Flexible}/S_{Rigid}$ = 1, indicating the situation with no effect of intrinsic flexibility. For each histogram the mean (μ) and standard deviation (σ) on $S_{Flexible}/S_{Rigid}$ are given.

Agrawal et al.[41] recently conducted similar studies for four different bulk mixtures containing equimolar mixtures of nonpolar adsorbates with similar sizes in 100 randomly chosen MOFs. At conditions in which the pores were highly loaded with adsorbing molecules, the mean and standard deviation of $\log(S_{Flexible}/S_{Rigid})$ from their simulations were -0.01 and 0.57, respectively. This indicates that, on average, the selectivities predicted with rigid structures were quite accurate, although there is considerable variation in this statement from case to case. Describing our data in the same logarithmic terms gives a mean (standard deviation) of 0.43 (0.30), 0.17 (0.22), and 0.20 (0.21) for sarin/H_2O, sarin/MeOH, and sarin/IPA mixtures, respectively. This indicates that unlike the results of Agrawal et al.[41] the mixtures of polar molecules of disparate sizes that we examined show systematic deviations between rigid and flexible structures, even on average.

3.3. Effect of Coulombic interactions of molecular mixtures

It is worthwhile to try to understand what aspects of the adsorbing molecules contribute the most to lack of quantitative agreement between simulations with rigid and flexible MOFs. The bulk mixtures we considered contain solvents that have distinct polarities and molecular sizes, but the results above cannot indicate which of these two factors plays a dominant role. To probe this issue, we performed simulations with unphysical nonpolar versions of each solvent by removing the point charges from each solvent molecule. Identical binary GCMC simulations as described above were carried with these unphysical solvent models for rigid and flexible MOFs. These simulations used the same partial pressures for each component as used above; we did not attempt to determine the effective vapor pressure of the unphysical solvents.

In Fig. 6, we repeated the same analysis as in Fig. 4 but using the unphysical nonpolar solvents in the GCMC simulations. Much, although not all, of the difference between the rigid and flexible results seen in Fig. 4 disappears when using the nonpolar solvents. This indicates that the polarity of adsorbing species, i.e. solvent, was much more responsible for the influence of framework flexibility than solvent size. The decreased sarin selectivity in intrinsically flexible MOFs when using nonpolar solvents occurs primarily because of lower sarin uptake rather than

changes in solvent loading relative to the rigid MOFs (see also Fig. S4). We note that Coulombic interactions in these molecular mixtures are not totally eliminated because the atomic point charges for sarin remained non-zero in these simulations.

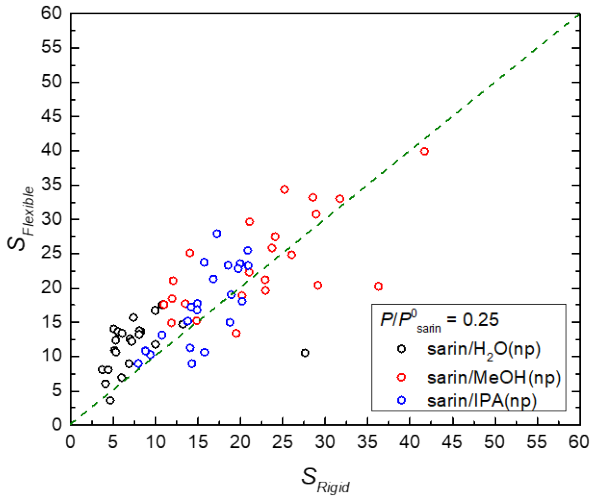

Fig. 6. Parity plot of adsorption selectivities predicted at 298 K in 23 MOFs approximated as rigid (horizontal axis) and allowed to have intrinsic flexibility (vertical axis) for each molecular mixture using unphysical nonpolar (np) solvents. The parity line indicates the result that would be obtained if there was no effect of intrinsic flexibility.

We revisit in Fig. 7 the histograms of $S_{Flexible}/S_{Rigid}$ after omitting the point charges on solvent molecules. Both μ and σ were significantly reduced in each binary mixture compared to those shown in Fig. 5. In agreement with Fig. 6, this indicates that solvent polarity is significantly more important than solvent size in determining the impact of framework flexibility on selective adsorption of sarin. The selectivity in the sarin/H_2O mixture, however, is still more sensitive to intrinsic flexibility than the other two mixtures. The difference in molecular sizes of sarin and the solvents is largest for sarin/H_2O and smallest for sarin/IPA (see Table S3). This implies that the impact of framework flexibility on adsorption can also be affected by the disparity in molecular size between adsorbing species. As an aside, we examined the effect of physical properties of MOFs, i.e. pore sizes, on the quantitative predictions of adsorption selectivity at rigid and flexible modes. We found the deviation between two predictions become more pronounced with small pore MOF materials (see Fig. S5).

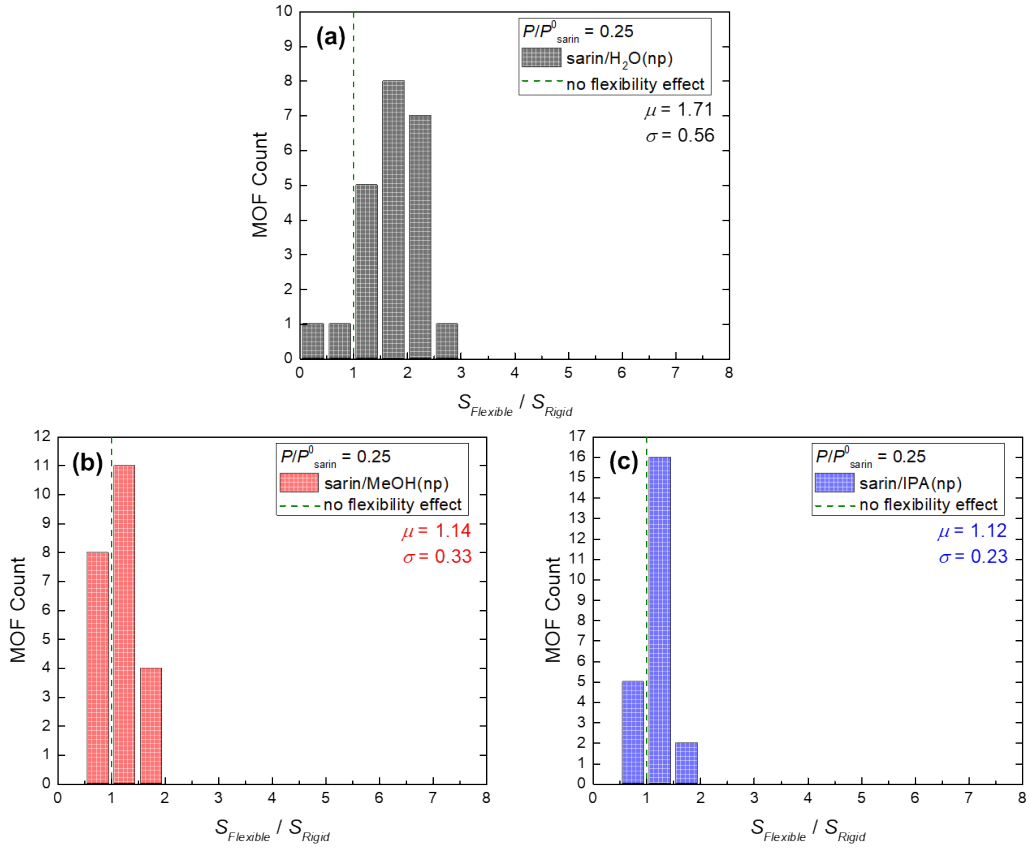

Fig. 7. Histogram plots showing the number of MOFs observed as a function of $S_{Flexible}/S_{Rigid}$ in each mixture of (a) sarin/H_2O, (b) sarin/MeOH, and (c) sarin/IPA using unphysical nonpolar (np) solvents. Green dashed lines show $S_{Flexible}/S_{Rigid}$ = 1, indicating the situation with no effect of intrinsic flexibility. For each histogram the mean (μ) and standard deviation (σ) on $S_{Flexible}/S_{Rigid}$ are given.

4. SUMMARY

In this article, we examined the adsorptive capture of sarin under bulk mixture adsorption conditions with aqueous and non-aqueous solvents in a collection of sarin-selective hydrophobic MOFs that were approximated as rigid and intrinsically flexible. Efficient catalytic degradation of sarin in MOFs in liquid environments can be feasible only if sarin is selectively adsorbed in the frameworks. Quantitative molecular modeling of adsorption, however, can be affected by including intrinsic flexibility that all porous materials indeed have by nature. Higher adsorption selectivity for sarin in non-aqueous solvents was predicted, both in rigid and intrinsically flexible MOFs, indicating that sarin detoxification using those solvents may be viable in properly chosen

MOFs when hydrolysis is incompatible. More importantly, we assessed the nontrivial deviation in adsorption properties predicted via rigid and intrinsically flexible MOFs. Our observations implied the impact of flexibility of this kind upon mixture adsorption is not negligible for mixtures containing polar adsorbates and adsorbates of disparate sizes. The computational methods we have used incorporate flexibility effects in the adsorbing materials, but neglect deformations of the adsorbent by the adsorbed species. It is computationally intensive to include these deformations[67-69], but doing so may be useful if calculations with our more efficient methods indicate a particular sensitivity to framework flexibility and high precision predictions are desired for specific adsorption conditions.

Our assessment of intrinsic framework flexibility effects for sarin separation has relied on a relatively small number of MOFs. Because the observed effects do not rely on special structural or chemical properties of the MOFs we considered, we anticipate that our observations may also apply to MOFs and porous materials more broadly. The viability of MOFs for CWA detoxification relies on both selective adsorption of CWAs and the catalytic activity of MOFs for adsorbed CWAs. Framework flexibility effects on catalytic activity is likely to be quite different than on adsorption, although the impact of these effects on adsorption hint that understanding the coupling between adsorbed CWAs, co-adsorbed solvent species and MOF frameworks may be important in achieving quantitative descriptions of this activity.

ASSOCIATED CONTENT

Electronic Supplementary Information

Electronic supplementary information (ESI) available:

MOF material set, adsorption conditions for solvents and mixtures, adsorption selectivity in rigid and intrinsically flexible MOFs, effect of MOF properties on quantitative predictions of adsorption selectivity, molecular modeling details, and numerical data for analysis.

AUTHOR INFORMATION

Corresponding Author

* E-mail: david.sholl@chbe.gatech.edu.

ORCID

Jongwoo Park: 0000-0002-8996-8362

Mayank Agrawal: 0000-0002-0331-5994

Dorina F. Sava Gallis: 0000-0001-6815-0302

Jacob A. Harvey: 0000-0002-5188-9036

Jeffery A. Greathouse: 0000-0002-4247-3362

David S. Sholl: 0000-0002-2771-9168

Notes

The authors declare no competing financial interest.

ACKNOWLEDGMENTS

This work is supported by the Academic Alliance at Sandia National Laboratories. Sandia National Laboratories is a multimission laboratory managed and operated by National Technology and Engineering Solutions of Sandia, LLC., a wholly owned subsidiary of Honeywell International, Inc., for the U.S. Department of Energy's National Nuclear Security Administration under contract DE-NA-003525. Any subjective views or opinions expressed herein do not necessarily represent the views of the DOE or the U.S. Government.

REFERENCES

1 F. R. Sidell, *Clin. Toxicol.*, 1974, **7,** 1-17.

2 R. T. Delfino, T. S. Ribeiro and J. D. Figueroa-Villar, *J. Braz. Chem. Soc.*, 2009, **20,** 407-428.

3 K. Kim, O. G. Tsay, D. A. Atwood and D. G. Churchill, *Chem. Rev.*, 2011, **111,** 5345-5403.

4 K. Vellingiri, L. Philip and K. H. Kim, *Coord. Chem. Rev.*, 2017, **353,** 159-179.

5 Y. Liu, A. J. Howarth, N. A. Vermeulen, S. Y. Moon, J. T. Hupp and O. K. Farha, *Coord. Chem. Rev.*, 2017, **346,** 101-111.

6 G. W. Peterson and G. W. Wagner, *J. Porous Mater.*, 2014, **21,** 121-126.

7 J. E. Mondloch, M. J. Katz, W. C. Isley III, P. Ghosh, P. Liao, W. Bury, G. W. Wagner, M. G. Hall, J. B. DeCoste, G. W. Peterson, R. Q. Snurr, C. J. Cramer, J. T. Hupp and O. K. Farha, *Nat. Mater.*, 2015, **14,** 512-516.

8 C. Montoro, F. Linares, E. Quartapelle Procopio, I. Senkovska, S. Kaskel, S. Galli, N. Masciocchi, E. Barea and J. A. R. Navarro, *J. Am. Chem. Soc.*, 2011, **133,** 11888-11891.

9 Y. Liu, S. Y. Moon, J. T. Hupp and O. K. Farha, *ACS Nano*, 2015, **9,** 12358-12364.

10 C. V. Soares, G. Maurin and A. A. Leitao, *J. Phys. Chem. C*, 2019, **123,** 19077-19086.

11 I. Matito-Martos, P. Z. Moghadam, A. Li, V. Colombo, J. A. R. Navarro, S. Calero and D. Fairen-Jimenez, *Chem. Mater.*, 2018, **30,** 4571-4579.

12 M. Agrawal, D. F. Sava Gallis, J. A. Greathouse and D. S. Sholl, *J. Phys. Chem. C*, 2018, **122,** 26061-26069.

13 Y. J. Jang, K. Kim, O. G. Tsay, D. A. Atwood and D. G. Churchill, *Chem. Rev.*, 2015, **115,** PR1-PR76.

14 M. J. Katz, S. Y. Moon, J. E. Mondloch, M. H. Beyzavi, C. J. Stephenson, J. T. Hupp and O. K. Farha, *Chem. Sci.*, 2015, **6,** 2286-2291.

15 S. Y. Moon, Y. Liu, J. T. Hupp and O. K. Farha, *Angew. Chem., Int. Ed.*, 2015, **54,** 6795-6799.

16 S. Y. Moon, G. W. Wagner, J. E. Mondloch, G. W. Peterson, J. B. DeCoste, J. T. Hupp and O. K. Farha, *Inorg. Chem.*, 2015, **54,** 10829-10833.

17 M. R. Momeni and C. J. Cramer, *ACS Appl. Mater. Interfaces*, 2018, **10,** 18435-18439.

18 M. R. Momeni and C. J. Cramer, *Chem. Mater.*, 2018, **30,** 4432-4439.

19 M. R. Momeni and C. J. Cramer, *J. Phys. Chem. C*, 2019, **123,** 15157-15165.

20 M. L. Mendonca and R. Q. Snurr, *Chem. Eur. J.*, 2019, **25,** 9217-9229.

21 D. F. Sava Gallis, J. A. Harvey, C. J. Pearce, M. G. Hall, J. B. DeCoste, M. K. Kinnan and J. A. Greathouse, *J. Mater. Chem. A*, 2018, **6,** 3038-3045.

22 D. Mandal, K. Sen and A. K. Das, *J. Phys. Chem. A*, 2012, **116,** 8382-8396.

23 M. J. Katz, J. E. Mondloch, R. K. Totten, J. K. Park, S. T. Nguyen, O. K. Farha and J. T. Hupp, *Angew. Chem. Int. Ed.*, 2014, **53,** 497-501.

24 S. Wang, L. Bromberg, H. Schreuder-Gibson and T. A. Hatton, *ACS Appl. Mater. Interfaces*, 2013, **5,** 1269-1278.

25 J. Park, R. P. Lively and D. S. Sholl, *J. Mater. Chem. A*, 2017, **5,** 12258-12265.

26 J. Park, J. D. Howe and D. S. Sholl, *Chem. Mater.*, 2017, **29,** 10487-10495.

27 D. Tang, Y. Wu, R. J. Verploegh and D. S. Sholl, *ChemSusChem*, 2018, **11,** 1567-1575.

28 S. Keskin and D. S. Sholl, *J. Phys. Chem. C*, 2007, **111,** 14055-14059.

29 C. Altintas, G. Avci, H. Daglar, A. Nemati Vesali Azar, S. Velioglu, I. Erucar and S. Keskin, *ACS Appl. Mater. Interfaces*, 2018, **10,** 17257-17268.

30 T. Duren, Y. S. Bae and R. Q. Snurr, *Chem. Soc. Rev.*, 2009, **38,** 1237-1247.

31 F. X. Coudert and A. H. Fuchs, *Coord. Chem. Rev.*, 2016, **307,** 211-236.

32 J. R. Li, Y. G. Ma, M. C. McCarthy, J. Sculley, J. M. Yu, H. K. Jeong, P. B. Balbuena and H. C. Zhou, *Coord. Chem. Rev.*, 2011, **255,** 1791-1823.

33 S. Keskin, J. Liu, R. B. Rankin, J. K. Johnson and D. S. Sholl, *Ind. Eng. Chem. Res.*, 2009, **48,** 2355-2371.

34 G. Ferey and C. Serre, *Chem. Soc. Rev.*, 2009, **38,** 1380-1399.

35 J. H. Lee, S. Jeoung, Y. G. Chung and H. R. Moon, *Coord. Chem. Rev.*, 2019, **389,** 161-188.

36 B. R. Pimentel, M. L. Jue, E. K. Zhou, R. J. Verploegh, J. Leisen, D. S. Sholl and R. P. Lively, *J. Phys. Chem. C*, 2019, **123,** 12862-12870.

37 A. Gladysiak, K. S. Deeg, I. Dovgaliuk, A. Chidambaram, K. Ordiz, P. G. Boyd, S. M. Moosavi, D. Ongari, J. A. R. Navarro, B. Smit and K. C. Stylianou, *ACS Appl. Mater. Interfaces*, 2018, **10,** 36144-36156.

38 M. Witman, S. Ling, S. Jawahery, P. G. Boyd, M. Haranczyk, B. Slater and B. Smit, *J. Am. Chem. Soc.*, 2017, **139,** 5547-5557.

39 M. Witman, B. Wright and B. Smit, *J. Phys. Chem. Lett.*, 2019, **10,** 5929-5934.

40 J. A. Gee and D. S. Sholl, *J. Phys. Chem. C*, 2016, **120,** 370-376.

41 M. Agrawal and D. S. Sholl, *ACS Appl. Mater. Interfaces*, 2019, **11,** 31060-31068.

42 Y. G. Chung, J. S. Camp, M. Haranczyk, B. J. Sikora, W. Bury, V. Krungleviciute, T. Yildirim, O. K. Farha, D. S. Sholl and R. Q. Snurr, *Chem. Mater.*, 2014, **26,** 6185-6192.

43 D. Nazarian, J. S. Camp and D. S. Sholl, *Chem. Mater.*, 2016, **28,** 785-793.

44 J. A. Harvey, M. L. McEntee, S. J. Garibay, E. M. Durke, J. B. DeCoste, J. A. Greathouse and D. F. Sava Gallis, *J. Phys. Chem. Lett.*, 2019, **10,** 5142-5147.

45 J. A. Harvey, J. A. Greathouse and D. F. Sava Gallis, *J. Phys. Chem. C*, 2018, **122,** 26889-26896.

46 H. Demir, K. S. Walton and D. S. Sholl, *J. Phys. Chem. C*, 2017, **121,** 20396-20406.

47 P. Z. Moghadam, D. Fairen-Jimenez and R. Q. Snurr, *J. Mater. Chem. A*, 2015, **4,** 529-536.

48 R. T. Yang, *Gas Separation by Adsorption Processes*, Imperial College Press, London, 1987.

49 R. C. Reid, J. M. Prausnitz and T. K. Sherwood, *Properties of Gases and Liquids*, McGraw-Hill, New York, 1977.

50 D. E. Coupry, M. A. Addicoat and T. Heine, *J. Chem. Theory Comput.*, 2016, **12,** 5215-5225.

51 S. Plimpton, *J. Comput. Phys.*, 1995, **117,** 1-19.

52 T. Watanabe and D. S. Sholl, *Langmuir*, 2012, **28,** 14114-14128.

53 E. Haldoupis, T. Watanabe, S. Nair and D. S. Sholl, *ChemPhysChem*, 2012, **13,** 3449-3452.

54 D. Dubbeldam, S. Calero, D. E. Ellis and R. Q. Snurr, *Mol. Simul.*, 2016, **42,** 81-101.

55 D. Dubbeldam, A. Torres-Knoop and K. S. Walton, *Mol. Simul.*, 2013, **39,** 1253-1292.

56 A. K. Rappe, C. J. Casewit, K. S. Colwell, W. A. Goddard and W. M. Skiff, *J. Am. Chem. Soc.*, 1992, **114,** 10024-10035.

57 M. G. Martin and J. I. Siepmann, *J. Phys. Chem. B*, 1998, **102,** 2569-2577.

58 M. P. Allen and D. J. Tildesley, *Computer Simulation of Liquids*, Oxford University Press, New York, 1987.

59 B. A. Wells and A. L. Chaffee, *J. Chem. Theory Comput.*, 2015, **11,** 3684-3695.

60 T. A. Manz and D. S. Sholl, *J. Chem. Theory Comput.*, 2010, **6,** 2455-2468.

61 T. A. Manz and D. S. Sholl, *J. Chem. Theory Comput.*, 2012, **8,** 2844-2867.

62 T. Watanabe, T. A. Manz and D. S. Sholl, *J. Phys. Chem. C*, 2011, **115,** 4824-4836.

63 B. Widom, *J. Chem. Phys.*, 1963, **39,** 2808-2812.

64 J. A. Harvey, C. J. Pearce, M. G. Hall, E. J. Bruni, J. B. DeCoste and D. F. Sava Gallis, *Dalton Trans.*, 2019, **48,** 16153-16157.

65 J. Piantadosi, P. Howlett and J. Boland, *J. Ind. Manag. Optim.*, 2007, **3,** 305-312.

66 J. Park, H. O. Rubiera Landa, Y. Kawajiri, M. J. Realff, R. P. Lively and D. S. Sholl, *Ind. Eng. Chem. Res.*, 2020, DOI: 10.1021/acs.iecr.9b05363.

67 M. Agrawal, S. Bhattacharyya, Y. Huang, K. C. Jayachandrababu, C. R. Murdock, J. A. Bentley, A. Rivas-Cardona, M. M. Mertens, K. S. Walton, D. S. Sholl and S. Nair, *J. Phys. Chem. C*, 2018, **122,** 386-397.

68 P. Lin and C. M. Colina, *Curr. Opin. Chem. Eng.*, 2019, **23,** 44-50.

69 G. Kupgan, A. G. Demidov and C. M. Colina, *J. Membr. Sci.*, 2018, **565,** 95-103.

TOC GRAPHIC

We assess the nontrivial deviation in predicting the adsorption selectivity from bulk mixtures of complex molecules using nanoporous adsorbents approximated as rigid and intrinsically flexible.